Analytica Chimica Acta 1169 (2021) 338631

Contents lists available at ScienceDirect

Analytica Chimica Acta

journal homepage: www.elsevier.com/locate/aca

Development of an aptamer-based SPR-biosensor for the determination of kanamycin residues in foods

Ángela Écija-Arenas [a, 1], Eva-Maria Kirchner [b, 1], Thomas Hirsch [b], Juan Manuel Fernández-Romero [a, *]

[a] Departamento de Química Analítica, Instituto Universitario de Investigación en Química Fina y Nanoquímica (IUNAN), Universidad de Córdoba, Campus de Rabanales, Edificio Anexo "Marie Curie", 14071, Córdoba, Spain
[b] Institute of Analytical Chemistry, Chemo and Biosensors, University of Regensburg, 93040, Regensburg, Germany

HIGHLIGHTS

- A biosensor based on the use of specific aptamer biding have been developed.
- The aptamer was immobilized at the sensor surface using two types of graphene.
- Chemical vapor deposition graphene and reduced graphene oxide were compared as sustrate surface.
- The union of the analyte was monitored by surface plasmon resonance.
- The aptasensor was applied to the kanamycin determination in cow milk samples.

GRAPHICAL ABSTRACT

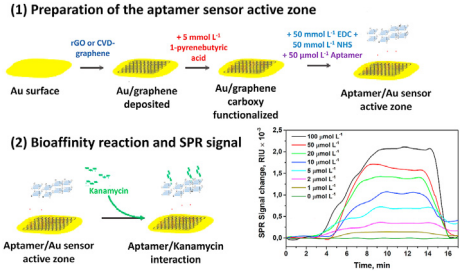

ARTICLE INFO

Article history:
Received 29 January 2021
Received in revised form
27 April 2021
Accepted 7 May 2021
Available online 11 May 2021

Keywords:
Aptamer sensor
Graphene support
Kanamycin residues detection
Surface plasmon resonance spectroscopy
Raman spectroscopy

ABSTRACT

A biosensor in which an affinity reaction occurs in the sensitive microzone through the use of specific aptamers to determine kanamycin residues in agri-food samples has been developed. It is an irreversible and continuous flow aptameric biosensor (aptasensor) in which the signal variations are monitored by surface plasmon resonance (SPR) measurements based on the specific interaction of the aptamer with the antibiotic. The signal variation is proportional to the analyte concentration. Graphene is known for efficient binding of molecules with its π-electron system, so a monolayer of graphene prepared from chemical vapor deposition (CVD) has been compared to a multilayer of graphene made from reduced graphene oxide (rGO) for immobilization of the aptamer on the gold surface of the physicochemical transducer. The best results have been obtained with CVD graphene. The dynamic range was between 1 and 100 µmol L^{-1} of kanamycin concentration ($r^2 = 0.9981$, n = 7, r = 4), with a limit of detection of 285 nmol L^{-1} and a sampling frequency of 6 h^{-1}. The precision, expressed as relative standard deviation (RSD%), was established in the range of 1.49 and 3.89%, calculated for 1, 10, and 50 µmol L^{-1}. The selectivity was studied applying the described method to determine other antibiotics, obtaining no significant difference in the analytical signal. The method was applied to determine kanamycin residues in milk samples with recovery values ranging between 90 and 96%.

* Corresponding author. Universidad de Córdoba, Campus de Rabanales, Edificio Anexo "Marie Curie", 14071, Córdoba, Spain.
E-mail address: qa1feroj@uco.es (J.M. Fernández-Romero).
[1] These authors contributed equally.

https://doi.org/10.1016/j.aca.2021.338631
0003-2670/

1. Introduction

Surface plasmon resonance (SPR)-based biosensors are valued in different fields such as medical diagnosis and analytical or biochemical monitorization for labeling-free and providing information on binding events in real-time monitoring methods [1–4]. SPR is an optical technique reporting an intensity change of the reflected light at a specific angle of incidence (resonance angle) at a receptor modified-metal surface caused by the alteration of the refractive index at proximity to this surface due to the analyte binding [5,6]. SPR sensing has been developed in the last years for timesaving, inexpensive, simple operation, and portable miniaturized devices [6,7]. Quantifying low molecular weight compounds makes this technique suitable for its application in broad areas such as clinical, pharmaceutics, theranostics, environmental research, and food safety [3,8]. It is widely used in real sample analysis due to the lack of matrix effect susceptibility, making sample pretreatment unnecessary. However, the sensitivity of the SPR sensor is determined by the sensor surface, considering the transport and binding of small concentrations of the analyte or the surface available for analyte binding. Approaches based on graphene coating of the gold substrate can improve the sensitivity and increase the immobilized molecule concentration [5].

Aptamers are short RNA or single-stranded DNA oligonucleotide sequences obtained by the *in-vitro* well-known selection process called SELEX (Systematic Evolution of Ligands by Exponential Enrichment). Their interest as recognition elements has been raised as an alternative to antibodies due to their high affinity and selectivity to the target molecule with the advantages of chemical stability, easy synthesis and modification, high resistance against denaturation, and ability to bind many types of target molecules, including antibiotics. These advantages make them attractive in the field of analytical chemistry, giving a new approach to biosensors. These types have been called aptasensors and have been used to determine a wide range of analytes with SPR detection [7,9,10]. Different options to assemble aptamers on the gold surface have been studied. Thiol groups self-assemble to the gold surface via well-known and stable Au—S-binding, so a thiol-modified aptamer can be developed [7,11,12]. Self-assembling via alkanethiols is known to form a too dense layer of aptamers, and the target cannot bind efficiently for steric hindrance and electrostatic reasons. This drawback can be overcome by diluting the aptamer-modified thiols with non-functionalized short-chain thiols at the surface, accompanied by an increase of non-specific binding. More advanced surface chemistry would enlarge the distance of the analyte to the surface. As sensitivity in SPR decays exponentially with distance, this is not favorable for reasons of decreased sensitivity. A feasible alternative is the use of graphene monolayers to anchor the aptamer to the surface.

Graphene is a 2D layered material of sp^2 hybridized carbon atoms with an increasing interest in the use of biosensors due to its properties, such as biocompatibility, high surface-to-volume ratio, π-stacking interactions, possible modifications, the presence of an intrinsic surface plasmon, and its hydrophobicity, which means there should be not much unspecific binding in aqueous systems. Graphene layers can be obtained multiple ways from top-down starting from graphite, like reduced graphene oxide (rGO), or bottom-up methods, like chemical vapor deposition (CVD) metal substrates. The first one was fabricated by chemical exfoliation as a top-down approach from graphite, and the second one was grown on a copper substrate. The physical and chemical properties of the resulting nanomaterial differed according to the adapted method, observing materials with different flake sizes and a different number of layers [13].

The rGO synthesis is simple, cheap, and the material can be processed quickly by drop-casting. Nevertheless, the preparation is time-consuming and cannot result in a large area of a uniform graphene monolayer. Thus, the resulting quality layer was not so excellent to increase sensitivity due to the considerable inhomogeneity and lattice defects. On the other hand, CVD results in an almost perfect monolayer with numerous receptor places and better sensitivity [7,14–16]. Both types of graphene have been used in biosensors to determine different analytes with SPR [5,6,14,17]. However, only the rGO has been used for kanamycin determination with various detection methods [18,19].

Once the aptasensor has been developed, its usefulness has been demonstrated by applying it to the determination of kanamycin residues in food samples. Kanamycin is an aminoglycoside antibiotic widely used in treating Gram-positive and Gram-negative bacterial infections in human and veterinary medicine due to the interaction with ribosomal RNA interfering with the bacterial protein synthesis [20,21]. However, kanamycin residues can be found in animal-derived foods due to their overuse. Accumulative overdose of this antibiotic may cause several affections such as nephrotoxicity, auditive loss, allergic reactions, and antibiotic resistance [22]. Therefore, the European Union has fixed maximum residue limits (MRLs) for kanamycin in milk as 150 $\mu g\ kg^{-1}$, and highly sensitive, accurate, economical, and simple detection methods have to be established to determine this amount [23].

In this study, an SPR-based biosensor was developed and applied to determine kanamycin by demonstrating the benefits of using CVD graphene compared to rGO. The differences between the two graphene types and the homogeneity of the transfer process were characterized using Raman spectroscopy.

2. Materials and methods

2.1. Reagents

Kanamycin sulfate from streptomyces kanamyceticus, penicillin, streptomycin, 1-pyrenebutyric acid (PBA), 1-ethyl-3-(3-(dimethylamino)propyl)carbodiimide (EDC), N-hydroxysuccinimide (NHS), and 16-mercaptohexadecanoic acid (MHA) were obtained from Sigma-Aldrich (Taufkirchen, Germany, www.sigmaaldrich.com). Other chemicals were obtained from VWR International (Darmstadt, Germany, www.de.vwr.com), and all chemicals used were of analytical grade. A solution containing 25 mmol L^{-1} disodium hydrogen phosphate (Merck, Taufkirchen, Germany, www.sigmaaldrich.com), adjusted to a pH 7.4, was used as the buffer. Kanamycin aptamer (5′—H_2N—AGATGGGGGTTGAGGCT-3′) was purchased from Eurofins Genomics (Ebersberg, Germany, www.eurofinsgenomics.eu) which is synthesized using SELEX procedure [18,24]. The aptamer was functionalized with an amino group at the 5' terminal for immobilization on the graphene surface. Before being used, the aptamer was stored at −4 °C ant in stock buffer (Eurofins Genomics, Germany) and was dissolved in the immobilization buffer containing 25 mmol L^{-1} disodium hydrogen phosphate, 100 mmol L^{-1} NaCl, and 4 mmol L^{-1} EDTA (pH 7.4), previous to its use.

2.2. Materials and instruments

Glass slides (20 × 20) mm of F1-type with a refractive index of 1.61 covered with a continuous gold film of 45 nm thickness were purchased at Mivitec GmbH (Sinzing, Germany, www.mivitec.de). Samples of a chemical vapor deposited graphene monolayer (10 × 10) mm grown on an 18 μm thickness copper substrate coated with approximately 60 nm thickness of a polymethylmethacrylate layer (PMMA) Model 495K, A2, which was purchased from Graphenea (San Sebastián, Spain, www.graphenea.com).

All SPR experiments were carried out on a BioSuplar SPR instrument (Mivitec GmbH, Germany). The gold-coated glass slide was brought in optical contact with an index-matching fluid (Cargille®, Cargille Labs, Cedar Groove, NJ, www.cargille.com). The solutions entered the system through a four channels peristaltic pump IPC 4 (Ismatec, NeoLab, Heidelberg, Germany, www.ismatec.com). Raman spectroscopy measurements used to characterize the subsequent sensor surface modification stages were performed on a DXR Raman microscope (Thermo Fisher Scientific GmbH, Dreieich, Germany, www.thermofisher.com). The Raman microscopic mapping images were obtained with an MPlan N 100'/0,90 BD objective (Olympus SE & Co. KG, Hamburg, Germany, www.olympus-europa.com).

2.3. Aptasensor fabrication

The aptasensor consisted of a glass slide covered with a thin gold layer and was functionalized with graphene to ensure the binding of the aptamer to the sensor surface. Two types of graphene were studied to carry out this binding, rGO, and CVD-graphene. Despite the graphene being directly deposited onto the sensor surface, a cleaning step must be introduced beforehand. The sensor surface formed by the gold-covered glass slides was thoroughly cleaned with ethanol and dried with a nitrogen stream.

The rGO was synthesized by a modified Hummers method and subsequent chemical reduction using hydrazine [25,26]. The gold-layer surface modification with rGO was developed by adapting a previously described method [27]. Gold surfaces were immersed in 16-mercaptohexadecanoic acid (MHA) before the rGO deposition to render the hydrophilic surface to improve their spreading adhesion to form a self-assembled monolayer (SAM) [28–30]. The slides have been immersed for a minimum of 20 h in an ethanolic solution of MHA (200 μmol L^{-1}). At ambient conditions, drop-casting of 50 μL rGO (β = 250 μg mL^{-1}) dispersed in a 1:1 (v/v) water and isopropanol solution ensured a uniform film formation on top of the slides.

CVD-graphene was grown by the direct deposition of gaseous reactants onto a substrate surface (Graphenea, Spain). For the modification with a monolayer of CVD-graphene, a wet transfer method was used [5,16]. CVD-graphene, supported by a copper substrate and covered by protective polymethylmethacrylate (PMMA) layer (Graphenea, Spain), was floated for 30 min on the surface of a solution of 400 μmol L^{-1} iron (III) chloride to etch the copper. After a thorough washing step, the CVD-PMMA-layer is deposited onto the slide, putting this one at the bottom of the solution and removing the solution to lower the film onto the gold slide. A thermal treatment consisted of heating at 70 °C in the air for 30 min flattened the CVD graphene film. The immersion of the slide into an acetone bath for 30 min is used to dissolve PMMA before the aptamer immobilization. The chips were rinsed with ethanol and dried with nitrogen.

Once the gold film was covered by graphene, the surface was modified with 1-pyrenebutyric acid (PBA) via π-stacking to ensure the covalent binding of the aptamer. PBA consists of a pyrene group molecule with π-electrons and a carboxylic group that can be used to facilitate further functionalization [15]. The graphene-modified slides were assembled into the flow system of the SPR instrument and treated with PBA. First, a 5 mmol L^{-1} PBA solution in DMSO was introduced into the system at a flow rate of 0.1 mL min^{-1} for 30 min. A carbodiimide coupling reaction ensured the binding of aptamers. EDC and NHS activated the carboxyl groups of PBA and facilitated an amide binding with the aptamer [31]. The buffer containing 50 mmol L^{-1} EDC and 50 mmol L^{-1} NHS was added at a flow rate of 0.2 mL min^{-1} for 10 min. The slide was incubated with 1 μmol L^{-1} antikanamycin aptamer dissolved in the immobilization buffer, containing 100 mmol L^{-1} NaCl and 4 mmol L^{-1} EDTA, for 30 min. Afterward, the slides were rinsed thoroughly with the buffer.

2.4. Aptasensor characterization

Besides the deposition of PBA, the quality of the deposited graphene films was monitored by Raman spectroscopy using a 532 nm laser excitation (10 mW) and with a 50 μm slit. SPR monitored the deposition of PBA and the aptamer. Changes in the intensity of reflected light were recorded at a fixed angle. An F1-65° glass prism was installed on a swiveling carriage. A flow cell with two channels was placed on the slide. One channel was used as a reference and the other one for the sample. Only the buffer, without analyte or surface modifiers, passed through the reference channel.

2.5. Kanamycin determination using the SPR based aptasensor

The determination of kanamycin is based on the affinity interaction between the analyte and the immobilized aptamer, which provides changes in the refractive index at the near-field surface monitored by an SPR detector. The SPR instrument includes two monitoring cells (reference and sample) that provide continuous monitoring of the refractive index variations at the same incidence angle close to the active sensor surface. The corrected baseline was obtained by subtracting the reference channel signal from the sample channel signal to eliminate small fluctuations in laser intensity or temperature variations. Any changes can be related only to the binding events at the sensor surface. The determination of kanamycin through the affinity interaction to the immobilized aptamer was studied at a concentration range between 1 and 100 μmol L^{-1} prepared in phosphate buffer (25 mmol L^{-1}, pH 7.4) at room temperature.

The selectivity of the aptasensor has been tested using an aminoglycoside antibiotic (streptomycin) and others from another antibiotic family (penicillin). The cross-reactivity of these antibiotics was tested at two concentrations (50 and 100 μmol L^{-1}) of each potential interferent.

2.6. Application of the method

The developed aptasensor was applied to determine different kanamycin concentrations in commercial cow milk samples (1.5% fat content) provided from a local commercial market. No sample pre-treatment was required to obtain the measurements, and samples were directly measured with the developed aptasensor. No kanamycin residues were found in previous studies performed with these milk samples. Therefore, a standard addition method was carried out with milk samples directly spiked with solid kanamycin to obtain a recovery study. Different kanamycin amounts were directly added to the samples to obtain known analyte concentration levels in samples ranged from the lowest concentration in the dynamic range to the middle of this range (1, 10, and 50 μmol L^{-1}). When their signal difference in RIU of each spiked sample was obtained regarding blank samples and the calibration graph, the added kanamycin concentration was calculated. The relation between the obtained and the known concentrations were necessary to obtain the recovery data.

3. Results and discussions

3.1. Aptasensor design and characterization

Several steps have been studied to obtain the best aptasensor signal. The first step is to functionalize the gold surface with both

graphene types (rGO and CVD-graphene). Fig. 1 depicted the Raman spectroscopy characterization. As can be seen, three Raman bands at 1350 cm^{-1} (D-peak), 1600 cm^{-1} (G-peak), and 2690 cm^{-1} (2D-peak) were used to identify the graphene layers. Intensity ratios between the characteristic bands, such as I_D/I_G and I_{2D}/I_G ratios, were used to indicate the graphene deposition on the metal surface. The ratio $I_{2D}/I_G \approx 2$ reveals the monolayer CVD deposition, whereas the low intensity of the 2D-peak of rGO shows stacked multilayers of graphene. The constant I_D/I_G ratio indicated the homogeneous distribution of reduced graphene oxide along the surface. This result was also attributed to the slide modified by CVD, as demonstrated by a constant I_{2D}/I_G ratio for CVD graphene due to the absence of a D-peak in CVD. The I_D/I_G ratio provides information about the flake size and some defects, involving the I_{2D}/I_G ratio with the number of layers [32,33].

In the case of rGO immobilization, different amounts of graphene were drop cast. The functionalized surfaces were analyzed using Raman microscopy (Fig. 2). The microscopic image with a 2D-intensity map of a characteristic peak (G-peak) (Fig. 2a) shown qualitative information about the film homogeneity. The continuous red color of the images indicates no variations in the layer thickness of the rGO deposited. Spectra of rGO (Fig. 2b) showed quantitative results with the typical features: broad peaks and, most importantly, an I_D/I_G ratio that is slightly higher than 1 [34]. The optimization of the influence of the amount of graphene used to perform the rGO deposition was supported on the I_D/I_G ratios obtained, shown in Table 1. The best results were achieved using 50 μL of a solution of 250 μg mL^{-1} rGO with 1:1 (v/v) isopropanol and water.

Regarding the immobilization of CVD graphene, Table 1 summarizes the intensity ratios studied. The presence of a small single 2D-peak with around double the G-peak intensity and an I_D/I_G ratio in the range of 0.05–0.3 is typical for CVD-derived monolayer samples [35]. These results indicate the successful transfer of CVD graphene onto the substrates.

The consecutive functionalization steps were monitored via Raman spectroscopy and SPR spectroscopy, depicted in Figs. 3 and 4. The graphene surface was modified using PBA via π-stacking interactions to facilitate the immobilization of the biorecognition molecules. PBA provided enough superficial acid groups on the modified graphene surface to facilitate the aptamer covalent bound through its amino-derived functionalization. As shown in Fig. 3, a small peak near the D-peak (1230 cm^{-1}) appeared on Raman due to the PBA deposition (red line) and possible G-peak intensity changes due to multilayer conversions. The I_{2D}/I_G ratio decreases from 2.19 ± 0.51 to 1.42 ± 0.23, keeping the I_D/I_G ratio constant in 0.18 ± 0.06. The SPR signal change expressed as refractive index units (RIU) has been used to monitor the SPR measurements. As shown in Fig. 4a, a change of $4 \cdot 10^{-3}$ RIU with CVD-graphene and $2.5 \cdot 10^{-3}$ RIU with rGO was obtained due to the immobilization of PBA.

The surface was modified with an EDC-NHS solution to activate the carboxyl groups and ensure binding to primary amines and the efficient coupling to the aptamer. After this modification, the Raman spectra remained constant. However, as shown in Fig. 4 b, the SPR signal changed to $2 \cdot 10^{-3}$ RIU using these EDC-NHS modified CVD-graphene surfaces and $1.6 \cdot 10^{-3}$ RIU EDC-NHS rGO. The I_{2D}/I_G ratio decreases again (1.25 ± 0.36) after the coupling of the antikanamycin aptamer, keeping constant the I_D/I_G ratio (0.17 ± 0.09) (blue line in Fig. 3). The refractive index changed to $1.8 \cdot 10^{-3}$ RIU for the CVD-graphene-based surface and $1.3 \cdot 10^{-3}$ RIU for the rGO-based (Fig. 4b). All this information suggests the successful modification of the graphene sensor with the biorecognition elements.

3.2. Analytical features of the method

The calibration graphs of the method for determining kanamycin using the aptasensor under the optimum experimental conditions and monitoring the SPR signal expressed in RIU are

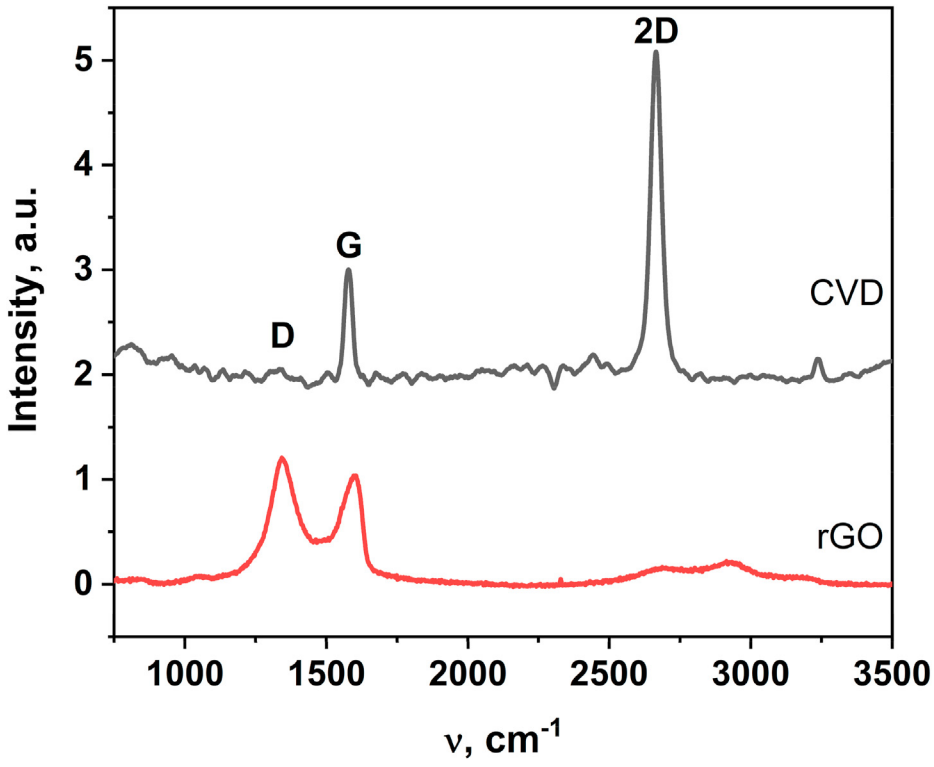

Fig. 1. Raman spectra of CVD-graphene and rGO modified slides normalized to the G-peak.

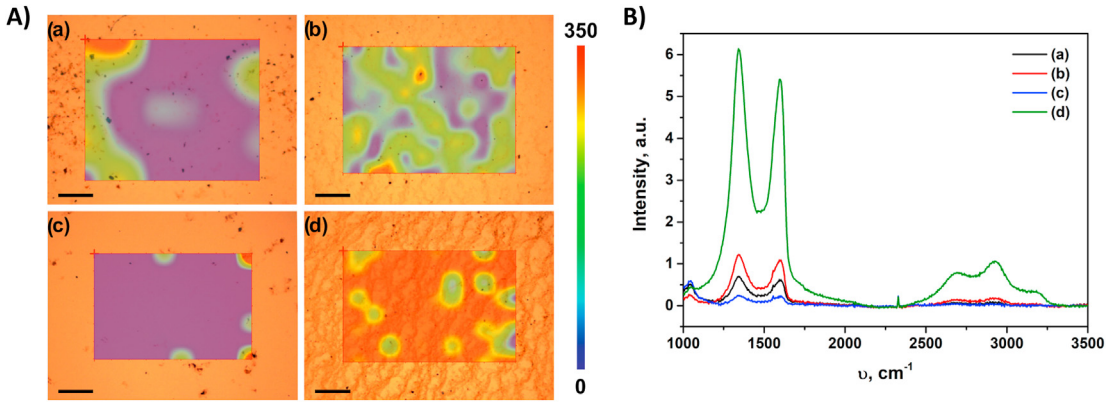

Fig. 2. Microscopic image (A) and Raman spectra (B) of a gold slide modified with 100 μL rGO (β = 62 μg mL^{-1}) (a), 50 μL rGO (β = 125 μg mL^{-1}) (b), 30 μL rGO (β = 250 μg mL^{-1}) (c), and 50 μL rGO (β = 250 μg mL^{-1}) (d). A 2D intensity map of the G-peak is blended over the microscopic images. The scale bars are 100 μm. (For interpretation of the references to color in this figure legend, the reader is referred to the Web version of this article.)

Table 1
I_D/I_G and I_{2D}/I_G ratios of each type of graphene used (n = 3, r = 50).

Type of graphene	Case number	I_D/I_G	I_{2D}/I_G
rGO			
100 μL of 62,5 μg mL^{-1} 1:4 (v/v) isopropanol and water	1	1.24 ± 0.28	0.39 ± 0.29
50 μL of 125 μg mL^{-1} 1:2 (v/v) isopropanol and water	2	1.12 ± 0.05	0.15 ± 0.07
30 μL of 250 μg mL^{-1} 1:1 (v/v) isopropanol and water	3	1.86 ± 0.51	0.67 ± 0.24
50 μL of 250 μg mL^{-1} 1:1 (v/v) isopropanol and water	4	1.14 ± 0.02	0.13 ± 0.03
CVD		0.14 ± 0.04	2.19 ± 0.51

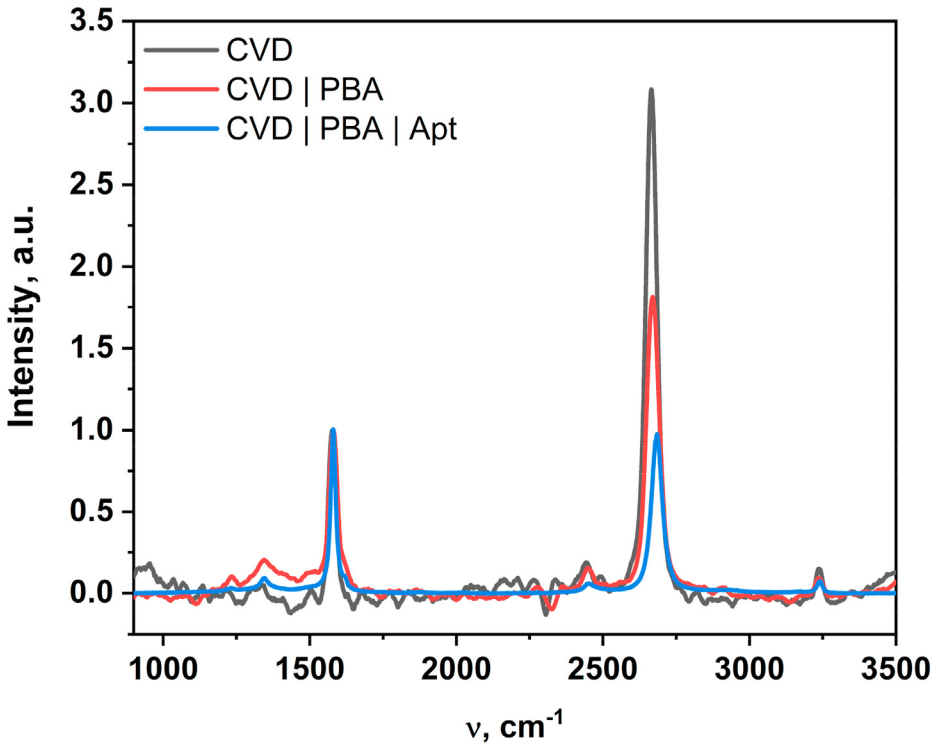

Fig. 3. Raman spectra of CVD modified slides (black line), CVD treated with 1-pyrenebutiric acid (PBA) (red line), and a CVD-PBA modified slide after the aptamer immobilization (blue line). (For interpretation of the references to color in this figure legend, the reader is referred to the Web version of this article.)

shown in Fig. 5. Fig. 5 a shows the RIU change for different kanamycin concentrations obtained with deposited CVD-graphene-based aptasensor. The SPR signal increased after the kanamycin binding, providing the immobilization of the antibiotic via the interaction with the specific aptamer, as evidenced in the calibration graphs in Fig. 5 b, where the difference between the signal

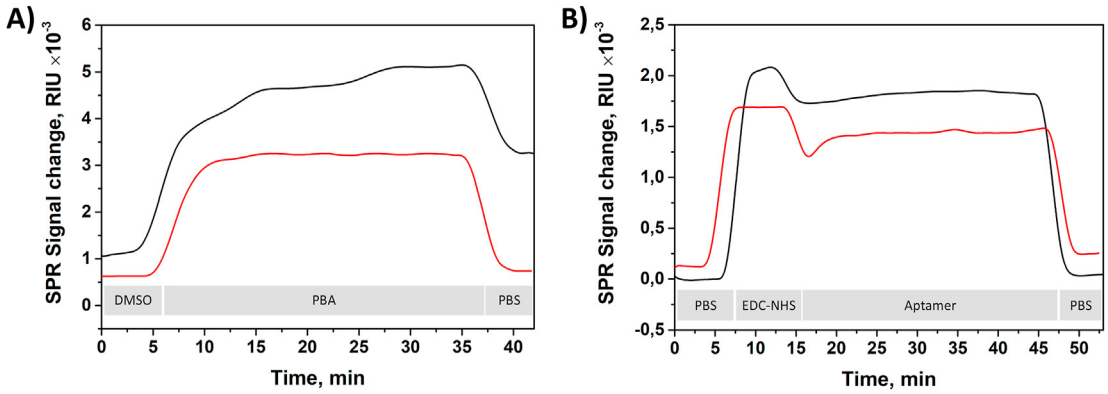

Fig. 4. SPR characterization of the gold surface with CVD-graphene (black line) and rGO (red line) after the immobilization of PBA (A) and the aptamer solution, with a previous modification with an EDC-NHS solution (B). (For interpretation of the references to color in this figure legend, the reader is referred to the Web version of this article.)

obtained when no kanamycin was bound to the aptasensor and the signal provided by different kanamycin concentration solutions has been represented. A linear relationship was found within the concentration mentioned above range, relating the difference signal with the kanamycin concentration logarithm.

Table 2 summarizes the features for the determination with rGO and CVD graphene, which include the equation parameters for the Hill relationship and the linearization of the representation, the dynamic range of the calibration graph, the limit of detection (LOD), and the limit of quantification (LOQ) established according to IUPAC recommendations [36], and the precision of the method expressed as RSD% values. LOD and LOQ were calculated from the standard deviation of the blanks. A high number of blanks ($r = 28$) were measured, and calculated the corresponding concentration for each calibration graph. Once concentrations were calculated, the mean and the standard deviation of the blank were obtained. LOD was defined by the mean value plus three times the standard deviation of the blank, and LOQ was obtained as the mean value plus ten times the standard deviation of the blank. The sampling frequency under the working conditions was estimated as 6 h^{-1}.

As can be seen, the LOD using CVD-graphene is round 0.28 μmol L^{-1}, which is 7-fold lower than obtained with rGO. The precision values were also better in the chase of the CVD-graphene aptasensor. The selectivity was studied by assaying other antibiotics (streptomycin and penicillin) instead of kanamycin. The results showed in Fig. 6 revealed that the kanamycin signal difference was significantly higher than other antibiotics.

The developed method based on an aptasensor has been compared with other methods for kanamycin or other aminoglycoside antibiotics determination. Several methods for determining kanamycin based on aptasensors [12,37–39] or SPR detection [40] separately have been established. Even though combining both techniques in the same method has been reported for determining other analytes [41], this combination has not been used to date for determining kanamycin. The LOD was in the same order of magnitude [42] or higher [38] than other methods based on luminescence detection but lower than using other aptasensors [39]. Nevertheless, the proposed method showed advantages concerning portability, cost, and measurement time. Also, the use of aptamers interaction provided higher selectivity than others supported on chemical reactions.

3.3. Application of the method

The developed aptasensor was applied to determine different kanamycin concentrations in commercial cow milk samples (1.5% fat content) from a local commercial market. No SPR signal response corresponding to kanamycin was observed when the milk samples were analyzed; thus, different kanamycin concentrations (1, 10, and 50 μmol L^{-1}) were directly added to the samples to carry out the standard addition method. A recovery study was carried out by adding kanamycin to reach three milk sample concentrations, obtaining their signal difference in RIU regarding blank samples. Taking into account the calibration graph, this difference was

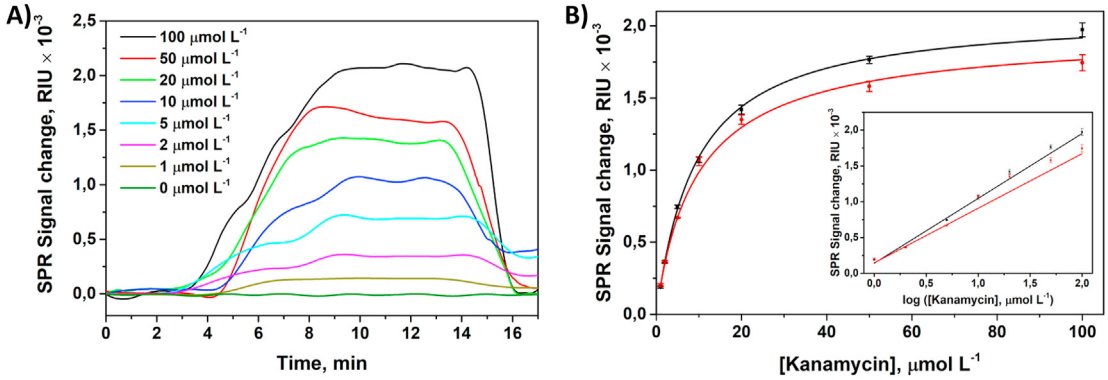

Fig. 5. (A) Signal change in refractive index units (RIU) of aptasensor with CVD-graphene with different kanamycin concentrations. (B) The derived relationship between the signal change in RIU of the aptasensor using CVD-graphene (black line) or rGO (red line) and the concentration of kanamycin. The inset indicates the linear relationship between the signal change in RIU and the logarithm of the kanamycin concentration for both types of graphene. (For interpretation of the references to color in this figure legend, the reader is referred to the Web version of this article.)

Table 2
Analytical features of the method.

	rGO method		CVD-graphene method	
Calibration graphs	Hill[a,b]	Linearization[a,c]	Hill[a,b]	Linearization[a,c]
Equation parameters	$RIU_{max} = 1.9 \cdot 10^{-3}$ ($\pm 6.5 \cdot 10^{-5}$) $K_D = 9.1$ (± 0.5) $r^2 = 0.997$	$a = 7.6 \cdot 10^{-4}$ ($\pm 5.8 \cdot 10^{-5}$) $b = 1.5 \cdot 10^{-4}$ ($\pm 3.9 \cdot 10^{-5}$) $r^2 = 0.967$	$RIU_{max} = 2.1 \cdot 10^{-3}$ ($\pm 3.4 \cdot 10^{-5}$) $K_D = 9.6$ (± 0.3) $r^2 = 0.998$	$a = 9.1 \cdot 10^{-4}$ ($\pm 5.1 \cdot 10^{-5}$) $b = 1.4 \cdot 10^{-4}$ ($\pm 2.8 \cdot 10^{-5}$) $r^2 = 0.982$
LOD, μmol L^{-1}	1.79	1.53	0.28	0.81
LOQ, μmol L^{-1}	5.88	3.46	0.92	1.06
Linear range, μmol L^{-1} (n = 7, r = 4)	5.88–100[d]	3.46–100	1–100[d]	1–100
RSD, % (r = 4)				
1 μmol L^{-1}	4.55		3.89	
50 μmol L^{-1}	1.26		1.49	

[a] y = signal difference in refractive index units (ΔRIU); x = kanamycin concentration (μmol L^{-1}).
[b] Hill equation: $y = RIU_{max} \cdot x/(K_D + x)$.
[c] Linearization of the representation: $y = a \cdot \log x + b$.
[d] Dynamic range for the Hill relationship.

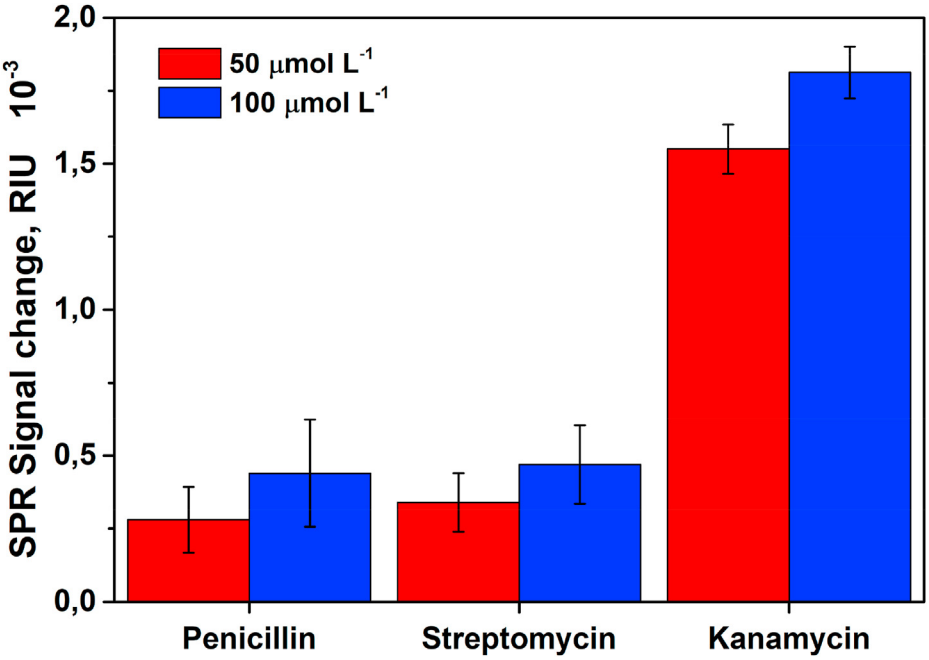

Fig. 6. Signal change in RIU for penicillin, streptomycin, and kanamycin at two concentration levels: 50 μmol L^{-1} (red columns) and 10 μmol L^{-1} (blue columns). (For interpretation of the references to color in this figure legend, the reader is referred to the Web version of this article.)

Table 3
Application of the method to the determination of kanamycin in milk.

Added, μmol L^{-1}	RIU signal[a]	Found[a], μmol L^{-1}	Recovery[a], %	RSD, % (n = 3)
1	$1.91 \cdot 10^{-4}$ ($\pm 1.44 \cdot 10^{-5}$)	0.96	96.24	7.55
10	$1.06 \cdot 10^{-3}$ ($\pm 9.52 \cdot 10^{-5}$)	9.78	97.85	5.91
50	$1.75 \cdot 10^{-3}$ ($\pm 4.71 \cdot 10^{-5}$)	45.06	94.53	2.72

[a] Mean value of three experiments.

related to the added kanamycin concentration. Known the added concentration, the recovery values were calculated. As can be seen in Table 3, the recovery values obtained were 96.24 ± 7.55%, 97.85 ± 5.91%, and 94.53 ± 2.72%, respectively for 1, 10, and 50 μmol L^{-1} kanamycin concentrations.

4. Conclusions

The development of SPR substrates based on graphene modified with aptamers has been carried out in this research and was applied to the determination of kanamycin residues. Comparing both types of graphene studied, rGO and CVD, the last one shows more homogeneous and reproducible graphene films, leading to a better immobilization of aptamers. Within SPR measurements, the highest surface sensitivity was achieved for those modified with CVD graphene, resulting in a 7-fold lower LOD for the kanamycin detection. Therefore, PBA can be attached to the 2D carbon nanomaterial via π-stacking and subsequently modified by the aptamer, leading to a universal approach for selective (bio)analysis. This feature represents an advantage in developing selective methods because just by changing the immobilized aptamer, the method can be adjusted to determine another analyte. The method has several

advantages, such as portability, speed of measurement, and low cost. The applicability of the method was demonstrated by the determination of one aminoglycoside antibiotic in milk samples. Even though the sensibility of the method and the values of LOD and LOQ can be improved to reach the values obtained with other techniques, the selectivity of the method was significant due to the high affinity and sensibility of aptamers for the target molecule.

CRediT authorship contribution statement

Ángela Écija-Arenas: Conceptualization, Data curation, Writing – original draft, Methodology, Formal analysis, Investigation, Writing – review & editing, Visualization. **Eva-Maria Kirchner:** Data curation, Resources, Supervision, Methodology, Writing – review & editing, Visualization. **Thomas Hirsch:** Conceptualization, Resources, Supervision, Methodology, Writing – review & editing, Project administration, Funding acquisition. **Juan Manuel Fernández-Romero:** Writing – review & editing, Project administration, Funding acquisition.

Declaration of competing interest

The authors declare that they have no known competing financial interests or personal relationships that could have appeared to influence the work reported in this paper.

Acknowledgement

This study is supported by the Operative Framework Funding FEDER-Andalucía 2014–2020 Program (ref. UCO-1263679). Á. Écija-Arenas thanks to the IDEP-UCO for the International Mobility Grant provided for her stay at the University of Regensburg.

References

[1] Z. Li, L. Leustean, F. Inci, M. Zheng, U. Demirci, S. Wang, Plasmonic-based platforms for diagnosis of infectious diseases at the point-of-care, Biotechnol. Adv. 37 (2019) 107440, https://doi.org/10.1016/j.biotechadv.2019.107440.
[2] M.M. Moussilli, A.R. El Falou, R.M. Shubair, Overview of fiber optic surface plasmon resonance biosensors for medical applications, in: Proc. - ANTEM 2018 2018 18th Int. Symp. Antenna Technol. Appl. Electromagn. 2018-Augus, 2018, pp. 12–13, https://doi.org/10.1109/ANTEM.2018.8572836.
[3] A. Jebelli, F. Oroojalian, F. Fathi, A. Mokhtarzadeh, M. de la Guardia, Recent advances in surface plasmon resonance biosensors for microRNAs detection, Biosens. Bioelectron. 169 (2020) 112599, https://doi.org/10.1016/j.bios.2020.112599.
[4] M. Bocková, T. Špringer, I. Nečasová, J. Nunvar, B. Schneider, J. Homola, Monitoring RAYT activity by surface plasmon resonance biosensor, Anal. Bioanal. Chem. 407 (2015) 3985–3993, https://doi.org/10.1007/s00216-015-8491-y.
[5] C. Genslein, P. Hausler, E.-M. Kirchner, R. Bierl, A.J. Baeumner, T. Hirsch, Detection of small molecules with surface plasmon resonance by synergistic plasmonic effects of nanostructured surfaces and graphene, in: Plasmon. Biol. Med., vol. XIV, 2017, p. 100800F, https://doi.org/10.1117/12.2252256.
[6] N.A.S. Omar, Y.W. Fen, S. Saleviter, W.M.E.M.M. Daniyal, N.A.A. Anas, N.S.M. Ramdzan, M.D.A. Roshidi, Development of a graphene-based surface plasmon resonance optical sensor chip for potential biomedical application, Materials 12 (2019), https://doi.org/10.3390/ma12121928.
[7] A. Blidar, B. Feier, M. Tertis, R. Galatus, C. Cristea, Electrochemical surface plasmon resonance (EC-SPR) aptasensor for ampicillin detection, Anal. Bioanal. Chem. 411 (2019) 1053–1065, https://doi.org/10.1007/s00216-018-1533-5.
[8] J.F. Masson, Surface plasmon resonance clinical biosensors for medical diagnostics, ACS Sens. 2 (2017) 16–30, https://doi.org/10.1021/acssensors.6b00763.
[9] W.W. Wang, X. Han, L.Q. Chu, Polyadenine-mediated immobilization of aptamers on a gold substrate for the direct detection of bacterial pathogens, Anal. Sci. 35 (2019) 967–972, https://doi.org/10.2116/analsci.19P110.
[10] W. Wu, Z. Zhu, B. Li, Z. Liu, L. Jia, L. Zuo, L. Chen, Z. Zhu, G. Shan, S.Z. Luo, A direct determination of AFBs in vinegar by aptamer-based surface plasmon resonance biosensor, Toxicon 146 (2018) 24–30, https://doi.org/10.1016/j.toxicon.2018.03.006.
[11] Y.S. Kim, J.H. Niazi, M.B. Gu, Specific detection of oxytetracycline using DNA aptamer-immobilized interdigitated array electrode chip, Anal. Chim. Acta 634 (2009) 250–254, https://doi.org/10.1016/j.aca.2008.12.025.
[12] H.Y. Song, T.F. Kang, N.N. Li, L.P. Lu, S.Y. Cheng, Highly sensitive voltammetric determination of kanamycin based on aptamer sensor for signal amplification, Anal. Methods. 8 (2016) 3366–3372, https://doi.org/10.1039/c6ay00152a.
[13] E.M. Kirchner, T. Hirsch, Recent developments in carbon-based two-dimensional materials: synthesis and modification aspects for electrochemical sensors, Microchim. Acta 187 (2020), https://doi.org/10.1007/s00604-020-04415-3.
[14] S. Szunerits, N. Maalouli, E. Wijaya, J.P. Vilcot, R. Boukherroub, Recent advances in the development of graphene-based surface plasmon resonance (SPR) interfaces, Anal. Bioanal. Chem. 405 (2013) 1435–1443, https://doi.org/10.1007/s00216-012-6624-0.
[15] M. Hinnemo, J. Zhao, P. Ahlberg, C. Hägglund, V. Djurberg, R.H. Scheicher, S.L. Zhang, Z. Bin Zhang, On monolayer formation of pyrenebutyric acid on graphene, Langmuir 33 (2017) 3588–3593, https://doi.org/10.1021/acs.langmuir.6b04237.
[16] J.W. Suk, A. Kitt, C.W. Magnuson, Y. Hao, S. Ahmed, J. An, A.K. Swan, B.B. Goldberg, R.S. Ruoff, Transfer of CVD-grown monolayer graphene onto arbitrary substrates, ACS Nano 5 (2011) 6916–6924, https://doi.org/10.1021/nn201207c.
[17] N.F. Chiu, C.T. Kuo, C.Y. Chen, High-affinity carboxyl-graphene oxide-based SPR aptasensor for the detection of hCG protein in clinical serum samples, Int. J. Nanomed. 14 (2019) 4833–4847, https://doi.org/10.2147/IJN.S208292.
[18] N.R. Ha, I.P. Jung, I.J. La, H.S. Jung, M.Y. Yoon, Ultra-sensitive detection of kanamycin for food safety using a reduced graphene oxide-based fluorescent aptasensor, Sci. Rep. 7 (2017) 1–10, https://doi.org/10.1038/srep40305.
[19] R. Li, Y. Liu, L. Cheng, C. Yang, J. Zhang, Photoelectrochemical aptasensing of kanamycin using visible light-activated carbon nitride and graphene oxide nanocomposites, Anal. Chem. 86 (2014) 9372–9375, https://doi.org/10.1021/ac502616n.
[20] N. Isoherranen, S. Soback, Chromatographic methods for analysis of aminoglycoside antibiotics, J. AOAC Int. 82 (1999) 1017–1045, https://doi.org/10.1093/jaoac/82.5.1017.
[21] L.S. Khabbaz, M. Hassanzadeh-Khayyat, P. Zaree, M. Ramezani, K. Abnous, S.M. Taghdisi, Detection of kanamycin by using an aptamer-based biosensor using silica nanoparticles, Anal. Methods. 7 (2015) 8611–8616, https://doi.org/10.1039/c5ay01807b.
[22] N. Zhou, J. Zhang, Y. Tian, Aptamer-based spectrophotometric detection of kanamycin in milk, Anal. Methods. 6 (2014) 1569–1574, https://doi.org/10.1039/c3ay41816b.
[23] Commision Regulation (EC), No 324/2004 of 25 February 2004 Amending Annex I to Council Regulation (EEC) No 2377/90 Laying Down a Community Procedure for the Establishment of Maximum Residue Limits of Veterinary Medicinal Products in Foodstuffs of Animal or, 2004.
[24] K.M. Song, M. Cho, H. Jo, K. Min, S.H. Jeon, T. Kim, M.S. Han, J.K. Ku, C. Ban, Gold nanoparticle-based colorimetric detection of kanamycin using a DNA aptamer, Anal. Biochem. 415 (2011) 175–181, https://doi.org/10.1016/j.ab.2011.04.007.
[25] W.S. Hummers, R.E. Offeman, Preparation of graphitic oxide, J. Am. Chem. Soc. 80 (1958) 1339, https://doi.org/10.1021/ja01539a017.
[26] A. Zöpfl, M.M. Lemberger, M. König, G. Ruhl, F.M. Matysik, T. Hirsch, Reduced graphene oxide and graphene composite materials for improved gas sensing at low temperature, Faraday Discuss 173 (2014) 403–414, https://doi.org/10.1039/c4fd00086b.
[27] C. Genslein, P. Hausler, E.M. Kirchner, R. Bierl, A.J. Baeumner, T. Hirsch, Graphene-enhanced plasmonic nanohole arrays for environmental sensing in aqueous samples, Beilstein J. Nanotechnol. 7 (2016) 1564–1573, https://doi.org/10.3762/bjnano.7.150.
[28] G. Yan, Y. Wang, X. He, K. Wang, J. Liu, Y. Du, A highly sensitive label-free electrochemical aptasensor for interferon-gamma detection based on graphene controlled assembly and nuclease cleavage-assisted target recycling amplification, Biosens. Bioelectron. 44 (2013) 57–63, https://doi.org/10.1016/j.bios.2013.01.010.
[29] C. Fenzl, C. Genslein, C. Domonkos, K.A. Edwards, T. Hirsch, A.J. Baeumner, Investigating non-specific binding to chemically engineered sensor surfaces using liposomes as models, Analyst 141 (2016) 5265–5273, https://doi.org/10.1039/c6an00820h.
[30] A.T. Reiner, N.G. Ferrer, P. Venugopalan, R.C. Lai, S.K. Lim, J. Dostálek, Magnetic nanoparticle-enhanced surface plasmon resonance biosensor for extracellular vesicle analysis, Analyst 142 (2017) 3913–3921, https://doi.org/10.1039/c7an00469a.
[31] C. Fenzl, P. Nayak, T. Hirsch, O.S. Wolfbeis, H.N. Alshareef, A.J. Baeumner, Laser-scribed graphene electrodes for aptamer-based biosensing, ACS Sens. 2 (2017) 616–620, https://doi.org/10.1021/acssensors.7b00066.
[32] A.C. Ferrari, J.C. Meyer, V. Scardaci, C. Casiraghi, M. Lazzeri, F. Mauri, S. Piscanec, D. Jiang, K.S. Novoselov, S. Roth, A.K. Geim, Raman spectrum of graphene and graphene layers, Phys. Rev. Lett. 97 (2006) 1–4, https://doi.org/10.1103/PhysRevLett.97.187401.
[33] C. Backes, K.R. Paton, D. Hanlon, S. Yuan, M.I. Katsnelson, J. Houston, R.J. Smith, D. McCloskey, J.F. Donegan, J.N. Coleman, Spectroscopic metrics allow in situ measurement of mean size and thickness of liquid-exfoliated few-layer graphene nanosheets, Nanoscale 8 (2016) 4311–4323, https://doi.org/10.1039/c5nr08047a.
[34] I.K. Moon, J. Lee, R.S. Ruoff, H. Lee, Reduced graphene oxide by chemical graphitization, Nat. Commun. 1 (2010), https://doi.org/10.1038/ncomms1067.

[35] L.M. Malard, M.A. Pimenta, G. Dresselhaus, M.S. Dresselhaus, Raman spectroscopy in graphene, Phys. Rep. 473 (2009) 51–87, https://doi.org/10.1016/j.physrep.2009.02.003.
[36] G.L. Long, J.D. Winefordner, Limit of detection: a closer look at the IUPAC definition, Anal. Chem. 55 (1983) 712A–724A, https://doi.org/10.1021/ac00258a001.
[37] R.Y. Robati, A. Arab, M. Ramezani, F.A. Langroodi, K. Abnous, S.M. Taghdisi, Aptasensors for quantitative detection of kanamycin, Biosens. Bioelectron. 82 (2016) 162–172, https://doi.org/10.1016/j.bios.2016.04.011.
[38] C. Liu, C. Lu, Z. Tang, X. Chen, G. Wang, F. Sun, Aptamer-functionalized magnetic nanoparticles for simultaneous fluorometric determination of oxytetracycline and kanamycin, Microchim. Acta. 182 (2015) 2567–2575, https://doi.org/10.1007/s00604-015-1628-z.
[39] X. Bai, H. Hou, B. Zhang, J. Tang, Label-free detection of kanamycin using aptamer-based cantilever array sensor, Biosens. Bioelectron. 56 (2014) 112–116, https://doi.org/10.1016/j.bios.2013.12.068.
[40] L. Zhang, C. Zhu, C. Chen, S. Zhu, J. Zhou, M. Wang, P. Shang, Determination of kanamycin using a molecularly imprinted SPR sensor, Food Chem. 266 (2018) 170–174, https://doi.org/10.1016/j.foodchem.2018.05.128.
[41] J. Ashley, S.F.Y. Li, An aptamer based surface plasmon resonance biosensor for the detection of bovine catalase in milk, Biosens. Bioelectron. 48 (2013) 126–131, https://doi.org/10.1016/j.bios.2013.04.009.
[42] Y. Zhang, P. Zuo, B.C. Ye, A low-cost and simple paper-based microfluidic device for simultaneous multiplex determination of different types of chemical contaminants in food, Biosens. Bioelectron. 68 (2015) 14–19, https://doi.org/10.1016/j.bios.2014.12.042.